

# Electron-Transfer Study and Solvent Effects on the Formal Potential of a Redox-Active Self-Assembling Monolayer

D. Acevedo and H. D. Abruña\*

Department of Chemistry, Baker Laboratory, Cornell University, Ithaca, New York 14853-1301  
(Received: May 16, 1991)

Solvent effects on the formal potential of the redox-active self-assembling system  $[\text{Os}(\text{bpy})_2(\text{dipy})\text{Cl}]^{1+}$  (bpy, 2,2'-bipyridine; dipy, 4,4'-trimethylenedipyridine) have been studied in six organic solvents and aqueous solutions. Cyclic voltammetry was used to determine surface coverage and formal potentials and the coulometric technique (charge injection) to determine double-layer capacitance. The variation of the formal potential with solvent and surface coverage is analyzed within the context of surface activity coefficients. The results seem to indicate that ion-pair formation between perchlorate anions (from supporting electrolyte) and the cationic head groups strongly influences the energetics of the system. An estimate of the standard rate constant for the electron transfer in aqueous solution reveals a very fast electron transfer with a lower limit of the order of  $10^5 \text{ s}^{-1}$ .

## Introduction

Electrochemical studies of self-assembling systems at electrodes can provide valuable information regarding the structure and composition of these films. Numerous investigators have employed electrochemical techniques to probe properties such as permeability, stability, and uniformity of these layers. Sagiv et al. employed cyclic voltammetry and impedance measurements to determine the presence of pinholes in self-organized layers of *n*-octadecyltrichlorosilane, octadecanethiol, and mixed monolayer films.<sup>1</sup> More recently, Finklea<sup>2</sup> and co-workers employed a fitting procedure of cyclic voltammograms to quantitatively characterize the size and distribution of pinholes in monolayers of octadecanethiol on gold electrodes. Capacitance measurements have been used by Chidsey and Loiacono to study the permeability of a series of thiols bonded to a gold surface having different functional groups facing the solution phase.<sup>3</sup> Cyclic voltammetry has been used extensively to probe the compactness of electroinactive self-organized layers by observing the electrochemical behavior of a suitable electroactive species in solution.<sup>4,5</sup>

In the case of electroactive self-assembling systems, the integrated charge under the voltammetric waves is usually taken as a direct measure of surface coverage.<sup>6-8</sup> From a knowledge of the surface coverage one can estimate an average projected area per molecule and propose models for the orientation of the molecules relative to the substrate surface. This method has been extensively employed in the determination of the orientation of adsorbed aromatic compounds at platinum electrodes.<sup>9</sup>

In this paper we present an electrochemical study of the redox-active self-assembling system  $[\text{Os}(\text{bpy})_2(\text{dipy})\text{Cl}]^{1+}$  (bpy, 2,2'-bipyridine; dipy, 4,4'-trimethylenedipyridine) (referred to as Osdipy in the text). In particular, we have studied variations in formal potential as the solvent and surface coverage were systematically varied, effects of the oxidation state of the monolayer on the double-layer capacitance, and electron transfer kinetics in aqueous solution.

A variety of electrochemical techniques were employed. Cyclic voltammetry was used to determine formal potentials and surface

coverage; fast cyclic voltammetry was employed to estimate the standard rate constant, and the coulometric technique (charge injection) was used for capacitance determination.

## Experimental Section

**Reagents.**  $\text{NaClO}_4$  (reagent grade, GFS Chemicals) was used as received. Water was purified by passing through a Milli-Q system and pyrolytic distillation (PDW). Tetra-*n*-butylammonium perchlorate (TBAP) (GFS Chemicals) was recrystallized three times from ethyl acetate and dried under vacuum at 75 °C for ~72 h. THF (Fisher) was distilled from sodium benzophenone. Acetonitrile, DMF, DMSO (Burdick & Jackson, distilled in glass), methylene chloride, and acetone (Fisher) were dried over 4-Å molecular sieves. The ligand 4,4'-trimethylenedipyridine (dipy) (Aldrich) was used as received. Perchloric acid (70%, Fisher) was of reagent grade.

**Instrumentation.** Voltammograms were obtained with a Princeton Applied Research Model 173 potentiostat and Model 175 universal programmer and recorded on a Hewlett Packard X-Y recorder. The fast cyclic voltammograms were obtained with a home-built potentiostat based on very fast (high bandwidth) operational amplifiers (LH0032 and LH0033) and recorded by using a Nicolet 4094 digital oscilloscope. The coulometric apparatus was home-built by using standard operational amplifier circuitry and PMOS switches (TL601, Texas Instruments). The overpotential-time transients were recorded by using a Nicolet 4094 digital oscilloscope.

**Synthesis of  $[\text{Os}(\text{bpy})_2(\text{dipy})\text{Cl}](\text{PF}_6)$ .**  $[\text{Os}(\text{bpy})_2\text{Cl}_2]$  (typically 200 mg) was heated at reflux and under nitrogen in thoroughly deaerated ethylene glycol (ca. 25 mL) for 3 h with 2 equiv of 4,4'-trimethylenedipyridine (dipy). The solution was allowed to cool; an equivalent volume of water was added, and the solution was subsequently filtered. The complex was precipitated by the addition of a saturated aqueous solution of  $\text{NH}_4\text{PF}_6$ . The complex was collected, washed with water, and dried with ether. Purification was carried out by chromatography on alumina with 15% methanol in toluene as eluent.

**Procedures.** The working electrode was a platinum disk sealed in glass. It was polished with 1  $\mu\text{m}$  diamond paste (Buehler) prior to use. Cleaning was carried out by cycling in 1.0 M  $\text{H}_2\text{SO}_4$  between the hydrogen adsorption and oxide formation regions until the characteristic voltammetry for a clean polycrystalline platinum electrode was obtained. From such a voltammogram, the microscopic area of the electrode was determined. The electrode was then rinsed with PDW and placed in 0.1 M  $\text{NaClO}_4$  solution (without the Osdipy complex) and cycled in the region of interest (typically between 0.0 and 0.5 V vs Ag/AgCl) until a steady (flat) background voltammogram was obtained. At this point the potential was held about 100–200 mV negative of the Osdipy wave

- (1) Sabatini, E.; Rubinstein, I.; Maoz, R.; Sagiv, J. *J. Electroanal. Chem.* **1987**, *219*, 365–371.
- (2) Finklea, H. O.; Snider, D. A.; Fedik, J. *Langmuir* **1990**, *6*, 371.
- (3) Chidsey, C. E. D.; Loiacono, D. N. *Langmuir* **1990**, *6*, 682.
- (4) Porter, M. D.; Bright, T. B.; Allara, D. L.; Chidsey, C. E. D. *J. Am. Chem. Soc.* **1987**, *109*, 3559–3568.
- (5) Finklea, H. O.; Robinson, L. R.; Blackburn, A.; Richter, B. *Langmuir* **1986**, *2*, 239–244.
- (6) Widrig, C. A.; Majda, M. *Anal. Chem.* **1987**, *59*, 754–760.
- (7) Miller, C. J.; Widrig, C. A.; Charych, D. H.; Majda, M. *J. Phys. Chem.* **1988**, *92*, 1928.
- (8) Lee, K. A. B. *Langmuir* **1990**, *6*, 709–712.
- (9) Hubbard, A. T.; Soriaga, M. P. *J. Am. Chem. Soc.* **1982**, *104*, 2735.

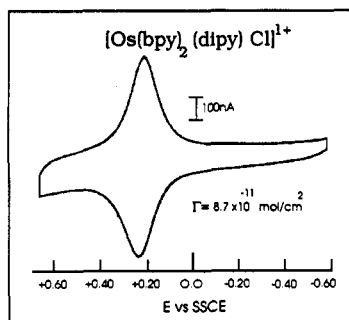


**Figure 1.** Cyclic voltammogram for adsorbed  $[\text{Os}(\text{bpy})_2(\text{dipy})\text{Cl}]^+$  in 0.1 M TBAP/ $\text{CH}_2\text{Cl}_2$ , at a polycrystalline platinum electrode; sweep rate = 100 mV/s.

(i.e., about 0.0 V vs Ag/AgCl) and the complex injected by microsyringe from an acetone solution of the complex (typically 0.5 mM). The injected volume varied depending on the desired final concentration of the complex. The system was allowed to reach equilibrium by waiting either 10–15 min or until the flow of charge had virtually stopped. This charge is due to the changing double-layer capacitance upon adsorption. Agitation of the solution (by purging with nitrogen) helps in accelerating the equilibration process. All solutions (except the acetone solution of Osdipy) were thoroughly deaerated with prepurified nitrogen.

After deposition was complete, the coverage was determined by cyclic voltammetry either in the same solution (the solution concentration of the complex, typically in the micromolar range, represents an insignificant fraction of the current) or, after the electrode was taken out of the deposition solution, rinsed with water/acetone, and transferred, to a solution containing only supporting electrolyte. For pH values below 5.0 the pH was adjusted by adding  $\text{HClO}_4$ . For pH values of 5.80 and 6.7 a phosphate buffer was used.

## Results and Discussions

**The System.** Before entering formally into the discussion, we shall describe the general voltammetry behavior of Osdipy and our reasoning leading to the model used throughout the discussion.

Figure 1 shows a cyclic voltammogram in methylene chloride (0.1 M TBAP) for a Pt electrode modified with about 0.9 monolayer (1 monolayer is  $1.0 \times 10^{-10}$  mol/ $\text{cm}^2$ ) of the Osdipy complex. The voltammetric shape is that anticipated for a surface-confined redox reagent. The redox process corresponds to a metal-based +2/+3 process. The adsorbed complex proved to be very stable (<10% loss after 15 min of continuous cycling at about 100 mV/s in aqueous solution), showing a very slow desorption if left in contact with a solution free of the complex. A very dilute aqueous solution ( $\sim 3 \mu\text{M}$ ) of the complex sufficed to maintain a saturation coverage. The complex is found to adsorb from organic solvents to a much lesser extent than in aqueous solution presumably because of higher solubility. The adsorption kinetics and its solvent dependence will be the subject of a future publication. However, once formed from aqueous solution, the films are stable in numerous organic solvents such as acetonitrile, methylene chloride, and other common solvents used in electrochemistry.

An isotherm at room temperature (22 °C) in aqueous solution is shown in Figure 2a. A very sharp rise, indicative of a large free energy of adsorption, is evident. There was little or no dependence on ionic strength (Figure 2b), but a strong dependence on pH was observed (Figure 2c). After the electrode was removed from the deposition solution (at a concentration on the saturation coverage plateau) and rinsed with water and acetone, voltammetry in clean supporting electrolyte was carried out. From integration of the charge under the voltammetric wave we obtained a coverage of  $1.0\text{--}1.2 \times 10^{-10}$  mol/ $\text{cm}^2$ . This is 10–20% smaller than the saturation coverage observed in the deposition solution (Figure 2b,c). This is likely due to a weak association of additional material after a monolayer is formed. This extra material is easily removed by the rinsing procedure. At the highest pH, oxide

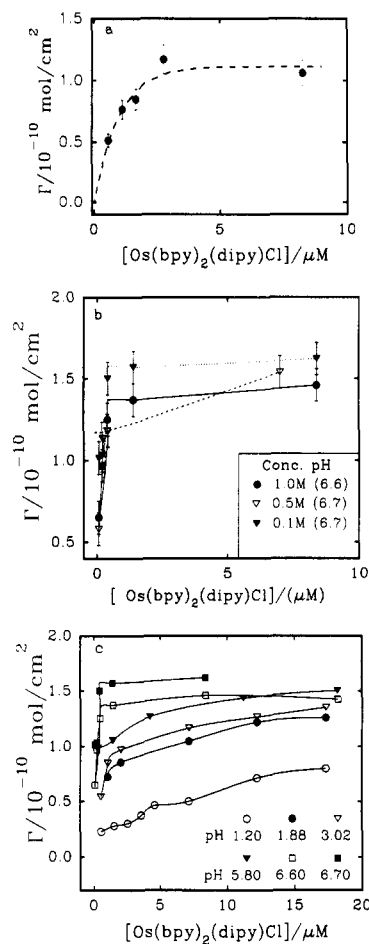


**Figure 2.** Room temperature isotherms for the adsorption of Osdipy on polycrystalline platinum electrodes from aqueous solution: (a) electrode was taken out from the deposition solution and rinsed with water/acetone prior to coverage determination; (b) coverage was determined in the deposition solutions containing various concentrations of supporting electrolyte ( $\text{NaClO}_4$ ) at constant pH; (c) coverage was determined in the deposition solutions at various pH values and constant supporting electrolyte concentration (0.1 M  $\text{NaClO}_4$ ). The error bars represent  $\pm 10\%$  of the corresponding value for the coverage. The lines through the symbols (except in part a) are spline fits.

formation and reduction contribute to the measured charge, so there is a larger uncertainty in these surface coverage measurements.

On the basis of the propensity of pyridine to adsorb to platinum, the strong dependence of the adsorption upon pH, and the value of the saturation coverage (see below), we postulate the mode of adsorption depicted in Figure 3. A molecular model reveals that the projected area of the Os moiety ( $[\text{Os}(\text{bpy})_2\text{Cl}]$ ) on the Pt surface is much bigger than that of the pyridyl group. If we consider the complex as a sphere with a radius of 7 Å (estimated by using van der Waals radii) attached to the surface by a rod (the dipy ligand), the calculated cross section per molecule ( $\sigma_m$ ) is  $154 \text{ Å}^2$ . This is in very good agreement with the experimental value of  $166\text{--}138 \text{ Å}^2$  obtained from the saturation coverage mentioned above. Of course, the same  $\sigma_m$  would have been obtained had the Os moiety been facing the electrode surface. However, we do not believe that this is the case since the complex  $[\text{Os}(\text{bpy})_2\text{pyCl}]^+$  (py, pyridine) does not show any propensity to adsorb.

**Capacitance Studies.** Initially, we sought to use the coulometric method (charge injection) to determine the standard rate constant. However, the double-layer relaxation was far too slow to allow a reliable measurement.<sup>10</sup> Instead, we used the technique to determine the double-layer capacitance. We used a home-built coulometric apparatus of similar design to that used by Brown and

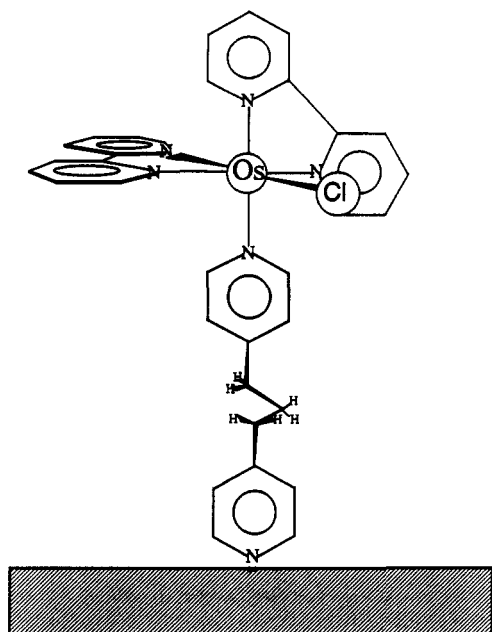


Figure 3. Schematic representation of the proposed mode of chemisorption of the Osdipy complex onto a platinum electrode showing the interaction of the free pyridinyl group with the electrode surface.

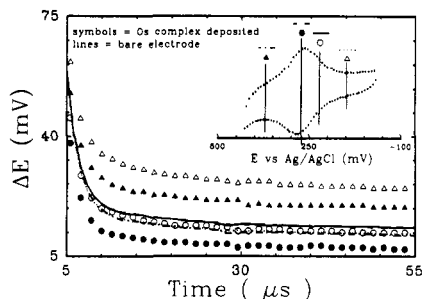


Figure 4. Overpotential-time transients recorded at various initial potentials covering the range for the oxidation/reduction process of the Os center in Osdipy. The injected charge was  $-1.1$  nC.

Anson,<sup>11</sup> which allowed for the variation of the initial potential prior to injection.

In the absence of any faradaic process, an injected charge  $\Delta q$  flows into the double-layer capacitance ( $C_{dl}$ ) causing an overpotential ( $\eta_\infty$ ) given by

$$\eta_\infty = \Delta q / C_{dl} \quad (1)$$

The ratio of two such overpotentials represents the ratio of the reciprocals of the corresponding double-layer capacitances, i.e.

$$\eta_\infty^\alpha / \eta_\infty^\beta = C_{dl}^\beta / C_{dl}^\alpha \quad (2)$$

where  $\alpha$  and  $\beta$  represent two different conditions such as two different potentials.

Figure 4 shows experimental overpotential-time transients for the bare and modified electrodes. The double-layer capacitance for the bare electrode does not change appreciably over the potential range under study. This is expected due to the high concentration of supporting electrolyte (0.1 M). Upon adsorption of the complex, there is an increase in the observed overpotential which corresponds (see eq 2) to a decrease in the double-layer capacitance by about a factor of 2. This is indicative of a compact layer formed at the expense of ionic displacement from the electrode/solution interface. More interesting is the observed increase ( $\sim 30\%$ ) in the double-layer capacitance when the change is made from a reduced to an oxidized layer. This effect might reflect a higher degree of ionic permeability for the more densely charged oxidized layer.

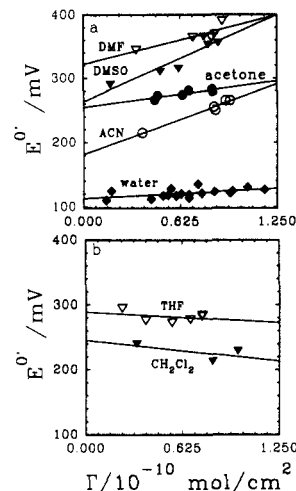


Figure 5. Variation of the formal potential ( $E^0$ ) for Osdipy with surface coverage and solvent.

TABLE I: Experimental Values of  $E_{sl}^0$ ,  $E_{so}^0$ , and  $E_{sol}^0$  (See Text) in millivolts vs SSCE Reference Electrode

solvent	$E_{sl}^0$	$E_{so}^0$	$E_{sol}^0$
THF	285	289	300
$\text{CH}_2\text{Cl}_2$	229	246	273
DMSO	355	263	300
DMF	390	322	338
acetone	281	255	290

**Variation of Formal Potential with Coverage and Solvent.** In the surface activity theory of Brown and Anson<sup>12</sup> for the case of immobilized molecules, the anodic and cathodic peak potentials are equal and related to the surface concentration by

$$E_{\text{peak}} = E^0 + (RT/nF)(r_R - r_O)\Gamma_T \quad (3)$$

where  $r_R$  and  $r_O$  are interaction parameters representing intermolecular interactions among reduced and oxidized forms, respectively (provided that the mixed interactions, i.e., ox-red and red-ox, are the same). In reality, the two peak potentials are not exactly equal and we will take the average ( $E^0$ ) to represent  $E_{\text{peak}}$  in eq 3. Thus, this theory predicts that the formal potential will shift depending on the relative magnitude of  $r_R$  and  $r_O$  as we change the surface coverage.

Figure 5 shows the variation of  $E^0$  in seven different solvents as a function of surface coverage. With the exception of THF and methylene chloride, all of them show a positive slope. According to eq 3, this means that either  $r_O$  is more negative than  $r_R$  (if both are negative) or  $r_R$  is more positive than  $r_O$  (if both are positive). However, from the voltammogram, the observed  $\Delta E_{\text{fwhm}}$  is, in all cases, larger than the ideal value of 90.6 mV (ranges from 100 to 135 mV), indicating repulsive (destabilizing) interactions which imply negative interaction parameters.<sup>12,13</sup> This is in accordance with expectations since we are dealing with a positively charged layer (+1 in reduced form, +2 in oxidized form) where the repulsions in the oxidized form are larger than in the reduced form. Qualitatively, one can say that the oxidation becomes easier as the system is more dilute due to the decrease in Coulombic repulsions among the headgroups. This trend in  $E^0$  seems to imply the formation of a uniformly spread layer at low coverage rather than separate islands of locally denser aggregates.

It is revealing to look at the behavior of  $E^0$  with solvent. In particular, we concentrate on three potentials representing three distinct states of the layer:  $E_{sl}^0$  is the formal potential of Osdipy on the surface at full monolayer coverage ( $\sim 1.0 \times 10^{-10}$  mol/cm<sup>2</sup>),  $E_{so}^0$  is the formal potential at "infinite dilution" as obtained from

(12) Brown, A. P.; Anson, F. C. *Anal. Chem.* **1977**, *49*, 1589.

(13) Smith, D. F.; Willman, K.; Kuo, K.; Murray, R. W. *J. Electroanal. Chem.* **1979**, *95*, 217.

(11) Brown, A. P.; Anson, F. C. *J. Electroanal. Chem.* **1978**, *92*, 133.

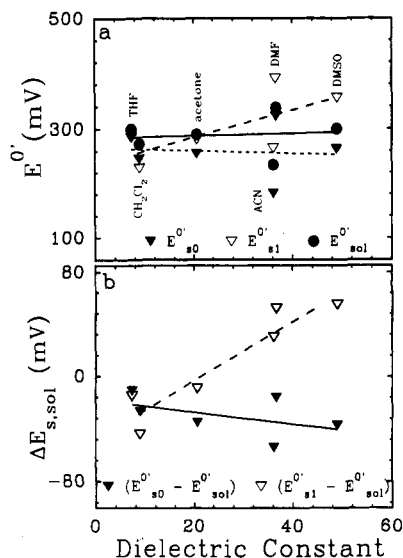


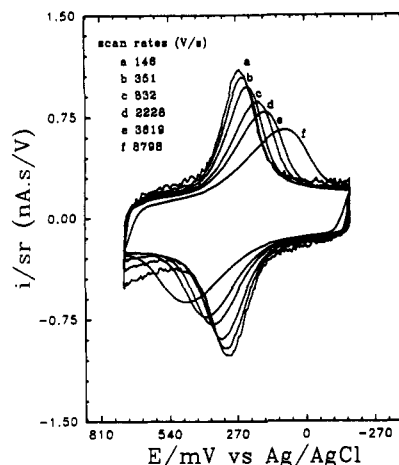
**Figure 6.** Variation of  $E^0_{s0}$ ,  $E^0_{s1}$ , and  $\Delta E_{s,sol}$  with dielectric constant (see text). All potentials are vs the SSCE reference electrode.

the intercept at  $\Gamma = 0$  in Figure 5, and  $E^0_{sol}$  is the corresponding formal potential in solution. These values are summarized in Table I. We select the parameter  $\epsilon_s$  (static dielectric constant) to represent each one of the solvents. This is a natural choice since it is this solvent property that controls electrostatic interactions among the different ions.

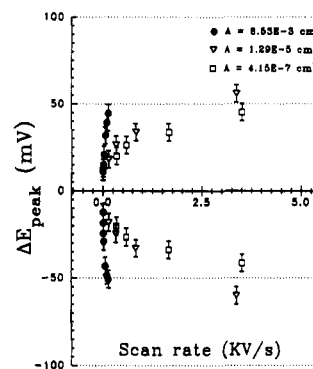
The solvent can modulate the intermolecular interactions in two complementary ways. The presence of solvent intercalated between headgroups results in a screening of the charge and thus suppresses the repulsion between sites. This diminution of the repulsion will be bigger for larger values of  $\epsilon_s$ . On the other hand, formation of ion pairs between, say, the perchlorate anions in solution and the charged headgroups on the surface would result in partial neutralization of the layer, therefore minimizing repulsion. This effect should be more pronounced at low  $\epsilon_s$ . The relative importance of these two solvent roles will depend strongly on the surface concentration of the Osdipy.

Figure 6a shows the variation of  $E^0_{s1}$ ,  $E^0_{s0}$ , and  $E^0_{sol}$  in different solvents (THF, acetone, acetonitrile, DMF, DMSO, methylene chloride), and as can be ascertained, a slightly stronger dependence is observed for the surface species. A more significant parameter for comparison is the difference between formal potentials for the surface and solution states. On taking this difference, we eliminate any variations in potential that might have been present during the measurements. Partial cancellation of specific solvent effects such as acidity and basicity (as expressed by Gutmann's donor and acceptor numbers) might also occur since they involve the interaction of the solvent with discrete molecules of the complex.<sup>14</sup> This quantity ( $\Delta E_{s,sol}$ ) emphasizes the intermolecular interactions on the surface using the solution as a reference state.

The results are plotted in Figure 6b. A very strong correlation is observed for the full monolayer case, whereas a much weaker dependence is present at infinite dilution. At full coverage, the ion-pair formation is maximized since the highest charge density exists. On the other hand, solvation is probably hindered as a result of the closed packed arrangement of the headgroups. Therefore, it appears that at full coverage ion-pair formation is more effective at minimizing the repulsion. At full coverage, the oxidation becomes easier (thermodynamically) as  $\epsilon_s$  decreases as evidenced by the increasingly less positive  $\Delta E_{s,sol}$ . This can be seen as a neutralization of the layer by ion pairing. If we diminish the formation of ion pairs by going to infinite dilution, the screening effect of the solvent should manifest itself and the slope of  $\Delta E_{s,sol}$  vs  $\epsilon_s$  should be opposite that for the above case. As depicted in Figure 6b, this is indeed the case. However, as we go to more and more dilute conditions, the distance between the headgroups



**Figure 7.** Cyclic voltammograms at various scan rates for a monolayer of Osdipy in 0.1 M  $\text{KClO}_4$  using a Pt microelectrode ( $A = 1.29 \times 10^{-5} \text{ cm}^2$ ).



**Figure 8.** Experimental  $\Delta E_{peak}$  vs scan rate for Osdipy in 0.1 M  $\text{KClO}_4$  at three different electrodes.

is already large and the repulsion weaker. This minimizes the importance of the screening mechanism and may account for the relatively mild dependence observed.

It is interesting to note that if we remove the intermolecular interactions on the surface, the formal potential is shifted negative relative to the solution potential. This is the case for solvents with very low dielectric constants (THF and methylene chloride), where the repulsion is neutralized by ion-pair formation, and at infinite dilution, where the separation of the headgroups is large.

**Electron Transfer.** Laviron<sup>15</sup> has derived general expressions for the linear potential sweep voltammetric response in the case of surface-confined species. From this formalism it is possible to determine the standard rate constant ( $k_s$ ) of electron transfer as well as  $\alpha$ , the transfer coefficient, by measuring the variation of peak potential with scan rate. However, this method is prone to large errors if one fails to consider the time constant of the cell, i.e.,  $R_u C_{dl}$ , where  $R_u$  is the uncompensated resistance and  $C_{dl}$  is the double-layer capacitance.

The utility of micro- and ultramicroelectrodes to minimize these errors has been recognized,<sup>16</sup> primarily for the case of heterogeneous electron transfer. However, they can also be employed in the study of electron-transfer kinetics of surface-confined species. The theory, use, and construction of ultramicroelectrodes have recently been reviewed.<sup>17</sup>

Voltammograms at various scan rates for adsorbed Osdipy in 0.1 M  $\text{KClO}_4$  using a platinum microelectrode (nominal 20- $\mu\text{m}$  diameter) are shown in Figure 7. The double-layer capacitance and uncompensated resistance were found to be 133 pF and 22 K $\Omega$ , respectively, as measured with the ac impedance method. This

(14) Scholl, H.; Sochaj, K. *Electrochim. Acta* 1988, 34, 915.

(15) Laviron, E. *J. Electroanal. Chem.* 1979, 101, 19.

(16) (a) Andrieux, C. P.; Hapiot, P.; Savéant, J. M. *J. Phys. Chem.* 1988, 92, 5987. (b) Andrieux, C. P.; Garreau, P. H.; Savéant, J. M. *J. Electroanal. Chem.* 1988, 248, 447. (c) Wipf, D. O.; Kristensen, E. W.; Deakin, M. R.; Wightman, R. M. *Anal. Chem.* 1988, 60, 306.

(17) Wightman, R. M.; Wipf, D. O. *Electroanal. Chem.* 1989, 15, 267.

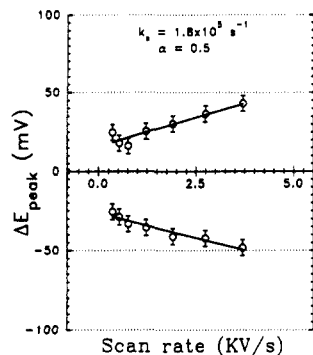


**Figure 9.** Experimental and theoretical variation of  $\Delta E_{\text{peak}}$  vs scan rate. For the calculation,  $\alpha = 0.5$ ,  $k_s = 1.8 \times 10^5 \text{ s}^{-1}$ ; experimental conditions were 0.1 M  $\text{KClO}_4$  and  $A = 4.14 \times 10^{-7} \text{ cm}^2$ .

value for the capacitance is an average one since, as mentioned under Capacitance Studies, it varies with the oxidation state of the monolayer. With this time ( $R_p C_d$ ) constant the maximum scan rate that can be employed with negligible distortion will be about 1400 V/s.<sup>18</sup> However, it is obvious from Figure 7 that very well defined voltammograms can be obtained at scan rates far larger than this limiting value.

To further check the validity of the above assertion, we carried out experiments with three different electrodes whose areas were  $8.53 \times 10^{-3}$ ,  $1.29 \times 10^{-5}$ , and  $4.15 \times 10^{-7} \text{ cm}^2$ , respectively. The resulting  $\Delta E$  ( $E_{\text{peak}} - E^0$ ) values for both the cathodic and anodic peaks are shown in Figure 8. Clearly, for the largest electrode, the error due to the cell time constant is intolerable even at relatively low scan rates. For the two smaller electrodes, however, the data compare very well for scan rates below 2500 V/s.

Figure 9 shows the experimental and theoretical  $\Delta E$  values as a function of scan rate for data obtained by using the smallest electrode ( $A = 4.15 \times 10^{-7} \text{ cm}^2$ ). The theoretical curve was calculated by using (see ref 15)  $\alpha = 0.5$  and  $k_s = 1.8 \times 10^5 \text{ s}^{-1}$ . This value of  $\alpha$  is only an approximation since for small  $\Delta E$  values the theoretical curve is relatively insensitive to  $\alpha$ .

It should be mentioned that the theoretical approach used here assumes a Langmuir isotherm, i.e., no interactions among the

adsorbed particles. However, as mentioned before, this does not appear to be the case in our system since the widths of the voltammetric peaks were larger than the ideal 90.6 mV. Thus, the value of  $k_s$  presented here should be taken to represent only an order of magnitude estimate of the actual standard rate constant. Nevertheless, it is clear that this is a very fast process.

### Concluding Remarks

With the combination of various electrochemical techniques, we have been able to extract kinetic and thermodynamic information about the redox-active self-assembling system consisting of monolayers (and submonolayers) of  $[\text{Os}(\text{bpy})_2(\text{dipy})\text{Cl}]^{1+}$  onto platinum electrodes. In particular, the coulometric technique provided a simple way to determine the double-layer capacitance which allowed us to monitor the ionic content within the monolayer. The variation of the formal potential with solvent and surface coverage as determined from cyclic voltammetry gave insightful information about the structure and energetics of this system.

The variation of the formal potential with coverage suggests the formation of a spread submonolayer (rather than islands of more concentrated aggregates) as the coverage decreases. From the variation of the difference in formal potentials of the surface-confined complex and solution complex with solvent (dielectric constant), we conclude that ion-pair formation between perchlorate anions and the charged layer of  $\text{Os}(\text{dipy})$  is, perhaps, the determining factor influencing the energetics of the redox process.

The use of micro- and ultramicroelectrodes allowed the use of very fast scan rates which in turn can yield values for the standard rate constant of electron transfer even for extremely fast processes such as the one studied here. Further work using microelectrodes is currently under way to explore solvent and surface coverage effects on the rate of electron transfer. A series of Os complexes with various dipyrilidyl ligands varying in length and degree of conjugation have been synthesized in our laboratory to further investigate the electron-transfer process in these monolayers.

**Acknowledgment.** D.A. acknowledges support by a MARC Fellowship of the National Institutes of Health. H.D.A. acknowledges support by the A. P. Sloan Foundation.

**Registry No.** THF, 109-99-9; ACN, 75-05-8; DMF, 68-12-2; DMSO, 67-68-5; TBAP, 1923-70-2;  $[\text{Os}(\text{bpy})_2(\text{dipy})\text{Cl}]^+$ , 136655-28-2;  $[\text{Os}(\text{bpy})_2(\text{dipy})\text{Cl}]\text{PF}_6$ , 136655-29-3;  $\text{NaClO}_4$ , 7601-89-0;  $\text{CH}_2\text{Cl}_2$ , 75-09-2;  $\text{HClO}_4$ , 7601-90-3;  $\text{KClO}_4$ , 7778-74-7; Pt, 7440-06-4; acetone, 67-64-1.

(18) Howell, J. O.; Kuhr, W. G.; Ensman, R. E.; Wightman, R. M. *J. Electroanal. Chem. Interfacial Electrochem.* **1986**, 209, 77.